

Mechanoradicals Created in “Polymeric Sponges” Drive Reactions in Aqueous Media**

H. Tarik Baytekin, Bilge Baytekin, and Bartosz A. Grzybowski*

The study of mechanochemical phenomena in polymers dates back to the work of Staudinger,^[1] who attributed the reduction in the molecular weight of polymers under mastication to the mechanical rupture of the constituent macromolecules. Subsequent studies have established that these and other related effects^[2] are a result of the homolytic cleavage of covalent bonds and creation of radicals within stressed polymers.^[3] Technologically, mechanochemical treatment has been used to adjust the rheological properties of rubbers,^[4] to degrade biopolymers, such as starch, to desired molecular weights,^[5] to dehalogenate hazardous polymer contaminants,^[6] to polymerize or copolymerize through vigorous milling and/or grinding, and it has also been used as the basis of mechanochromism.^[7] Yet, these applications remain scarce and specialized, and in virtually all everyday systems where polymers are subject to mechanical stresses, for example, in the tires of road vehicles, the soles of walking shoes, and so on, the chemical energy of homolytically broken bonds is not being harnessed in any purposeful way. Herein, we show how a significant fraction of this ubiquitous, and in some sense “free” (for otherwise not used), energy can be retrieved if the polymers that are being deformed are in contact with water. Under these conditions, the mechanoradicals that are created within the polymer migrate to the polymer/water interface, at which they produce H_2O_2 , which can then drive several types of chemical processes, such as nanoparticle synthesis, dye bleaching, or fluorescence. The amount of H_2O_2 that is produced scales with the interfacial area and is in the order of tens of mg m^{-2} for 1 J of mechanical energy input, and the overall efficiency of the mechanical-to-chemical energy conversion is, depending on the polymer used, from approximately 7% up to a remarkable 30% for

soft, “spongy” polymers. Deformable polymer “sponges” that drive aqueous-phase radical reactions can be construed as solid-state chemical reagents that convert mechanical energy into chemical energy in a “clean”, environmentally friendly fashion. On the other hand, the fact that polymers under stress produce potentially harmful^[8] free radicals might raise concerns about the safety of polymer-based medical implants.^[9]

We used the flexible polymers poly(dimethylsiloxane) (PDMS, Dow Corning, Sylgard 184), Tygon (Saint-Gobain Corp. #R-3603), and poly(vinyl chloride) (PVC, VWR, #60985-534), all of which gave qualitatively similar results. Typically, hollow polymer tubes (inner diameter 0.6–0.8 cm, outer diameter 1.5 cm, height ca. 7.5 cm) were filled with water or an aqueous solution of a desired reagent, and were compressed mechanically with strains of up to 40% (Figure 1a). In all cases, the deformations were nondestructive and reversible at the macroscopic level, as shown by the force-displacement curves of the squeezed polymers not changing over many compression/release cycles (see Figure S10 in the Supporting Information). Measurements with a Faraday cup connected to a high-precision electrometer (Keithley, 6517B) confirmed that the compressed pieces did not generate any measurable static electricity (surface charge densities were

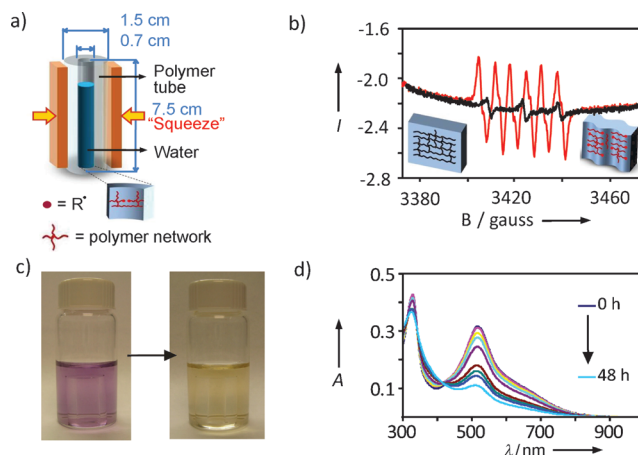


Figure 1. a) Tubes made of PDMS, Tygon, or PVC are filled with deionized water and are compressed by a vice. b) ESR spectrum of a solution of DMPO in THF (1 mg mL^{-1}) in the presence of compressed PDMS in an argon atmosphere (red) or uncompressed PDMS (black, the same spectrum is obtained in the absence of any PDMS). c) A solution of DPPH ($10.0 \mu\text{M}$) changes color from purple to yellow when squeezed polymer tubes (in this case, Tygon) are added, which indicates the transformation from DPPH into DPPH-R in the presence of radicals. d) The changes in the UV/Vis spectra of the solution of DPPH shown in (c) over time.

[*] Dr. H. T. Baytekin, Dr. B. Baytekin, Prof. B. A. Grzybowski
Department of Chemistry and Department of Chemical and
Biological Engineering, Northwestern University
2145 Sheridan Road, Evanston 60208 IL (USA)
E-mail: grzybor@northwestern.edu
Homepage: <http://dysa.northwestern.edu>

[**] This work was supported by the Non-equilibrium Energy Research Center (NERC) which is an Energy Frontier Research Center funded by the U.S. Department of Energy, Office of Science, Office of Basic Energy Sciences under Award Number DE-SC0000989. We would like to thank Prof. Michael R. Wasielewski and Dr. Tomoaki Miura for their help with ESR spectroscopy, Dr. Bartłomiej Kowalczyk for SEM imaging, Pat Fuller for his help in radical diffusion simulations, and Prof. Fraser J. Stoddart and Albert C. Fahrenbach for CV measurements. XPS spectrum was taken at the KECK-II facility at NU. H.T.B. and B.B. contributed equally to this work.

Supporting information for this article is available on the WWW under <http://dx.doi.org/10.1002/anie.201108110>.

below the detection limit of the electrometer, ca. 10 pC). On the other hand, mechanical deformation created radicals in the polymers. This finding agrees with previous studies^[3] and is directly shown by electron spin resonance (ESR) experiments. For example, Figure 1 b shows a typical ESR spectrum of PDMS immersed in a solution of the spin-trapping reagent 5,5-dimethylpyrroline-*N*-oxide (DMPO, necessary to stabilize the radicals at room temperature) in THF.^[10] If the piece of PDMS is not compressed, the ESR spectrum shows only the signals from DMPO. However, upon polymer deformation the spectrum changes dramatically and features a pattern with hyperfine coupling constants ($a_N = 1.29$ mT, $a_H = 0.68$ mT) that are characteristic of a spin adduct of DMPO with $\equiv\text{RO}\cdot$ ($\equiv\text{CO}\cdot$ and $\equiv\text{SiO}\cdot$) radicals.^[11] For PDMS, adducts that are compatible with the obtained spectra include those that originate from homolytic cleavage of Si–O bonds^[25] ($\equiv\text{SiO}\cdot$ or $\equiv\text{SiOO}\cdot$; from reaction of $\equiv\text{Si}\cdot$ with trace O_2) or the cleavage of Si–C and C–C bonds at the crosslinking points within the polymer,^[26] which give rise to $\equiv\text{SiO}\cdot$ or the peroxy radicals $\equiv\text{SiOO}\cdot$ or $\equiv\text{COO}\cdot$ from reaction of $\equiv\text{Si}\cdot$ and $\equiv\text{C}\cdot$ with O_2 in air under ambient conditions. The presence of radicals is also shown by bleaching of solutions of 2,2-diphenyl-1-picrylhydrazyl (DPPH) in the presence of compressed polymers (Figure 1 c,d). Importantly, if the polymers are not present or compressed, no bleaching is observed.

The key finding of the present study is that the radicals that are created by the homolytic cleavage of bonds in stressed polymers can react with the surrounding aqueous phase to generate H_2O_2 from water (Figure 2 a). This was verified in four independent ways: i) by the appearance of a characteristic H_2O_2 ^1H NMR signal^[12] at $\delta = 10.1$ ppm (Figure 2 b); ii) by the appearance of a UV absorption band between 200–300 nm^[13] (Figure 2 c); iii) by cyclic voltammograms that have a H_2O_2 reduction peak at around -0.4 V (versus Ag^+/AgCl reference electrode; Figure 2 d); and iv) by the so-called Fenton reaction,^[14] $\text{H}_2\text{O}_2 + \text{Fe}^{2+} \rightarrow \text{OH}^- + \text{Fe}^{3+} + \text{OH}\cdot$, which is dependent on the presence of H_2O_2 , and produces ferric ions that complex with a selective indicator, Xylenol Orange (XO),^[15] to give the absorption peak centered at 560 nm (Figure 2 e). It should be stressed that none of the characteristic features i)–iv) are detected in control experiments with nondeformed polymers. Also, the involvement of mechanoradicals is consistent with the finding that the amount of H_2O_2 produced decreases dramatically when the polymers being deformed are doped with antioxidants, such as α -tocopherol or bis(1-octyloxy-2,2,6,6-tetramethyl-4-piperidyl) sebacate (HALS),^[16] which are known to scavenge radicals.

With the above results in mind, a plausible mechanism for H_2O_2 synthesis is illustrated in Figure S1 in the Supporting Information, and involves various mechanoradicals $\text{R}\cdot$, $\text{RO}\cdot$ or $\text{ROO}\cdot$, which are generated in the polymer, reacting with water. We note that as the number of bonds strictly at the inner surface of a polymer tube is only on the order of approximately 10^{15} per cm^2 , the radicals that are generated at these locations alone cannot account for the production of approximately $5 \mu\text{M}$ of H_2O_2 (see below). It follows that the radicals generated in the bulk of the polymer, approximately 10^{16} radicals per cm^3 (see Section 2.2 in the Supporting

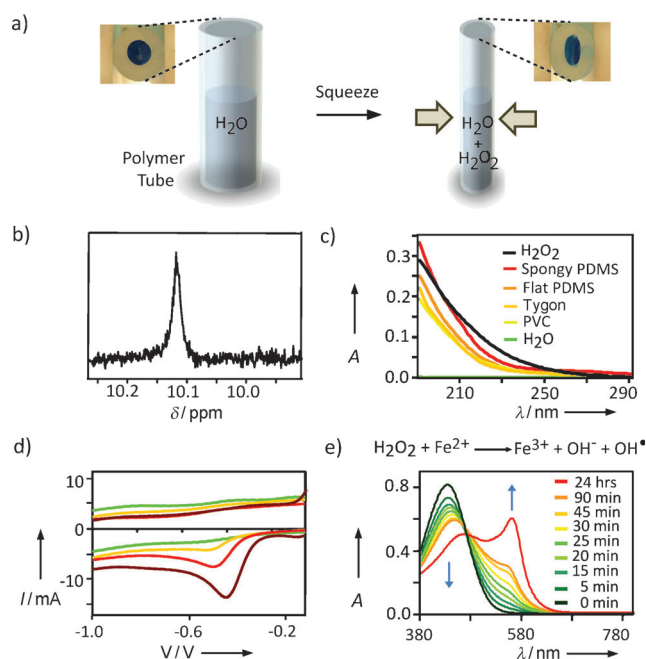


Figure 2. a) H_2O_2 is created by squeezing a polymer tube filled with water. Insets: top views of the unsqueezed and squeezed tube filled with a dye solution (for visualization). b) The ^1H NMR spectrum (400 MHz, D_2O) of H_2O_2 produced in deionized and argon-purged H_2O (3 mL) in a squeezed PDMS tube. The peak is absent before polymer squeezing. c) The UV/Vis spectra illustrate that H_2O_2 is generated by compression of polymer tubes. A spectrum of H_2O_2 (1.0 mM) is also shown for comparison (black). d) Cyclic voltammograms (sections from -1.0 V to -0.1 V) recorded during squeezing of a PDMS tube (red) containing deionized H_2O (3 mL). For comparison, voltammograms of pure water before squeezing (green) and standard H_2O_2 solutions (4 mM (yellow) and 40 mM (brown)) are shown. e) UV/Vis spectra recorded during the Fenton reaction ($(\text{NH}_4)_2\text{Fe}(\text{SO}_4)_2$ (25 μM) and XO (125 μM) in H_2SO_4 (20 mM)). The numbers next to the curves indicate the times for which spongy PDMS was compressed. The data for PDMS, PVC, and Tygon are qualitatively similar.

Information), should be able to migrate towards the surface of the polymer, possibly by a radical-driven propagation mechanism^[17] that is similar to that reported previously in mechanically treated poly(ethylene)^[18] (Figure S2 in the Supporting Information). This scenario is corroborated by the data shown in Figure 3 a, which shows the concentration of H_2O_2 that is produced in tubes over time after 5 min of compression. As time passes, more radicals from the bulk reach the polymer/water interface to produce H_2O_2 . Interestingly, as shown in Figure S5 in the Supporting Information, the concentration versus time dependencies for various polymers fit well to the diffusion equation, and the effective diffusion coefficients of the radicals in the polymer are on the order of $10^{-10} \text{ m}^2 \text{ s}^{-1}$.

If, as assumed, the production of H_2O_2 takes place at (or near) the polymer/water interface, the amount of H_2O_2 that is generated at a given time point should increase with increasing polymer surface area. To test this hypothesis, we performed several experiments. In one experiment, we fabricated “spongy” PDMS tubes that present a corrugated surface (see Section 1 in the Supporting Information for

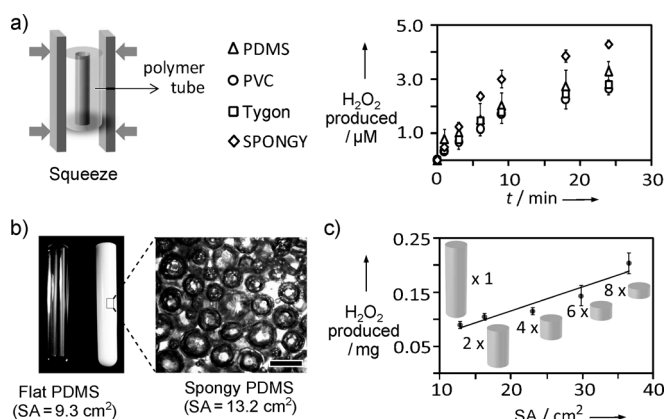


Figure 3. Kinetics of H_2O_2 production by squeezed polymers. a) Time-dependent concentration of H_2O_2 produced by squeezing PDMS (Δ), PVC (\circ), Tygon (\square), and spongy PDMS tubes (\diamond). Height of tubes = 2 cm, other dimensions same as described for Figure 1. The tubes were first compressed in air for 5 min and then fully immersed in Fenton test solution (10 mL XO ($50 \mu\text{M}$) and Fe^{2+} ions ($10 \mu\text{M}$) in aq. H_2SO_4 (2 mM)) for different times. b) Flat (left) and spongy PDMS tubes (right). The optical micrograph magnifies the sub-millimeter depressions at the surface of the spongy PDMS. SA = surface area; scale bar = $200 \mu\text{m}$. c) The amount of H_2O_2 produced versus the surface area of the compressed PDMS. In both (a) and (c), the amount of H_2O_2 produced was calculated by using a calibration curve derived from H_2O_2 standards of known concentration ($0.1 \mu\text{M}$ – $10 \mu\text{M}$). Error bars were obtained from four individual measurements.

fabrication details), the area of which is roughly 1.4 times that of “flat” PDMS tubes (Figure 3b). When the flat and the spongy tubes were each filled with 3 mL of water and compressed for 5 min each, the amount of H_2O_2 that was produced was $3.3 \mu\text{M}$ and $4.3 \mu\text{M}$, respectively (1:1.30 ratio). In another set of experiments, one, two, four, six, and eight pieces of PDMS with total surface area of 12.8 cm^2 , 16.2 cm^2 , 23.0 cm^2 , 29.8 cm^2 , and 36.6 cm^2 , respectively (total mass of the polymer kept constant in each experiment) were compressed 100 times in polyethylene bags filled with 10 mL water, for 15 min. The amounts of H_2O_2 produced in one squeeze cycle were on the order of 20 mgm^{-2} per 1 J of mechanical energy input, which is similar to other single-squeeze experiments. As illustrated in Figure 3c, the amount of H_2O_2 produced scaled linearly with the surface area (similar linear dependencies were obtained for the other polymers that were tested).

The quantities of mechanosynthesized H_2O_2 are sufficient to drive small-scale chemical syntheses. The idea of coupling the mechanochemical production of H_2O_2 to other chemical reactions is illustrated by the examples in Figure 4. In the first example (Figure 4a), an aqueous solution of a metal salt (for example, $\text{HAuCl}_4 \cdot 3\text{H}_2\text{O}$, typical concentration $c = 2 \text{ mg mL}^{-1}$) is fully reduced and deposits a thin (20–100 nm) layer of gold nanoparticles on the polymer surface (characterized by XPS lines $\text{Au}4f_{7/2}$ and $\text{Au}4f_{5/2}$ at 84 eV and 88 eV, respectively, and by the depletion of the salt from the solution). SEM and UV/Vis spectroscopic analyses show that the layer comprises spherical nanoparticles that measure 50 nm in diameter and have an SPR maximum at 537 nm

(note: the synthesis of silver nanoparticles was also achieved by similar means). In the second set of reactions, water-soluble organic redox dyes (Methylene Blue (MB) and Neutral Red (NR); $c = 2.5$ – $10 \mu\text{M}$) are bleached (Figure 4b; for MS analyses, see Figure S6 in the Supporting Information). The progress of bleaching was monitored by UV/Vis spectroscopy, in which the intensity of an internal charge-transfer band (from the donor dimethylamino group and the acceptor phenazine [NR] and thiazine [MB]^[19] with maxima at $\lambda = 535 \text{ nm}$ for NR and $\lambda = 664 \text{ nm}$ for MB) decreased gradually. Each time the polymer was squeezed, the reaction showed first-order kinetics (see Figure S7 in the Supporting Information). With consecutive squeezing events, the amount of the dye that was bleached in each cycle remained approximately constant (Figure 4b, right). In the third, and perhaps the most illustrative example, the compression of a shoe sole was coupled to the generation of fluorescent umbelliferone (7-hydroxycoumarin) from its boronic ester derivative. In this experiment, we injected a solution of the boronic ester derivative ($5 \mu\text{M}$ in aqueous phosphate buffer (0.1 M , pH 7.4)) into the sole cushion of a basketball shoe (Nike Air Max LeBron VII, Figure 4c). After walking for several tens of minutes, enough mechanoradicals and H_2O_2 were generated to cleave the boronic ester and produce umbelliferone, which fluoresced blue-green light ($\lambda_{\text{em}} = 454 \text{ nm}$) that was clearly visible to the naked eye upon irradiation with UV (365 nm) light.

We note that all of the above reactions do not occur in the presence of unsqueezed polymers and are congruent with the proposed mechanism in which radicals that are generated within the polymer react with water or oxygen to ultimately create hydroxyl and/or hydroperoxyl radicals in solution (Figure S1 in the Supporting Information, see also [20]). For instance, the synthesis of gold nanoparticles mediated by H_2O_2 has been reported,^[21] as has the radical oxidation of NR and MB dyes with H_2O_2 .^[22] The use of umbelliferone to detect H_2O_2 has also been described previously.^[23] Of course, there are many other chemical processes that can be driven mechanochemically. In upcoming publications, we will describe examples in which the mechanochemical production of H_2O_2 is coupled to more complex chemical systems and drives, for example, rotaxane shuttling, polymerization, or epoxidation of double bonds.

A crucially important parameter of any mechanosynthesis, and one that ultimately determines its practical applicability, is its energetic efficiency. In this study, we estimated it in two ways: i) based on the amount of H_2O_2 produced and ii) based on the number of radicals created. In the first case, the amount of H_2O_2 produced is estimated based on the UV/Vis spectra of the Fenton reaction (Figure 2e). In the second method, the number of radicals is determined from the UV/Vis spectra of the bleached DPPH solutions (Figure 1c,d). In both cases, it is assumed that the radicals that affect these reactions come from the mechanoradicals that are created by homolytic cleavage of bonds within the polymer (indeed, no Fenton reaction or DPPH bleaching occurs with unsqueezed polymers). Knowing the approximate numbers of bonds broken in the polymer and the average bond energies, one can then estimate the amount of chemical

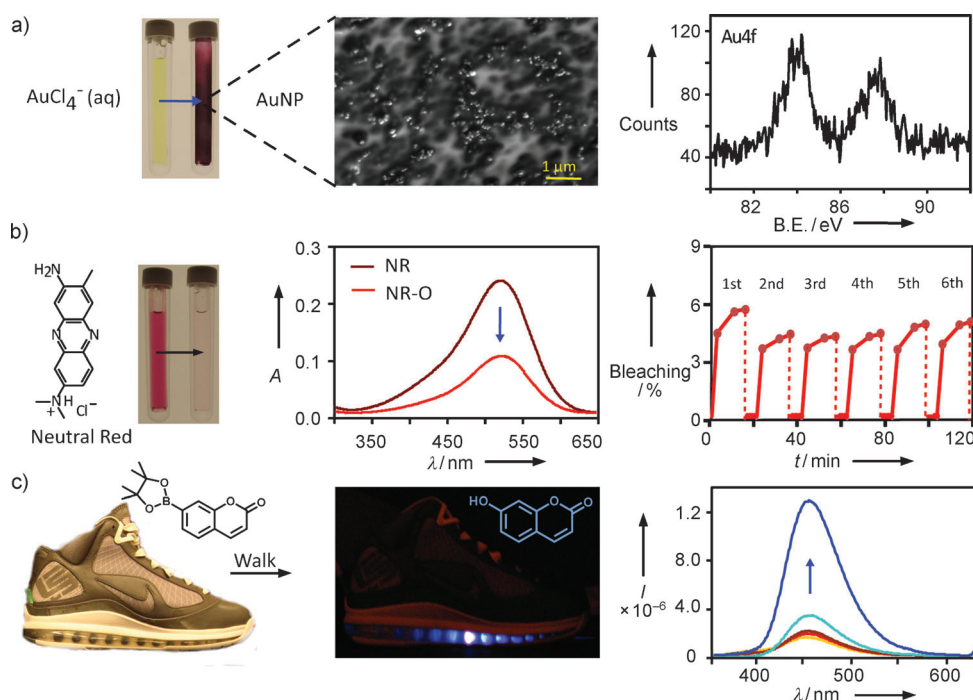


Figure 4. a) Reduction of gold(III) salt (2 mg mL^{-1}) to ca. 50 nm gold nanoparticles deposited on the inner surface of a PDMS tube (left), the corresponding SEM image (middle, scale bar = $1 \mu\text{m}$), and the corresponding high-resolution XPS spectrum (right). b) Oxidative bleaching of an aqueous solution of Neutral Red dye ($2.5 \mu\text{M}$ in pH 5.0 sodium acetate buffer) in a squeezed PVC tube (left), the corresponding UV/Vis spectrum (middle), and the reaction progress for six consecutive squeezing events (right). In each cycle, a new aliquot of the dye solution ($2.5 \mu\text{M}$ at pH 5.0) was introduced and a compressive strain of ca. 40% was applied. c) Fluorescent umbelliferone (middle) produced in solution by cleavage of a boronic ester derivative (left, 50 mL , $5.0 \mu\text{M}$ in phosphate buffer (0.1 M , pH 7.4)) in the voids of the sole of a shoe and fluorescence spectra recorded after 30 min (yellow), 45 min (red), 1 h (brown), 2 h (light blue) of walking and 24 h at rest after walking (dark blue).

energy released by polymer compression. To derive efficiency, this chemical energy is divided by the work expended while squeezing the polymer (for calculation details, see Figures S8 and S9 in the Supporting Information). This calculation is reminiscent of the definition of efficiency in a Carnot cycle (work done versus heat absorbed) and does not take into account the fact that most of the mechanical energy can be actually regained when compression ceases and the polymer expands (this could make efficiencies unrealistically high and the polymers should be then considered as energy sources rather than mechanical-to-chemical energy transducers). Importantly, both methods give similar estimates of efficiency that range from 4–12% for flat PDMS, Tygon, or PVC to a rather remarkable 30% for spongy PDMS, which is easier to compress and offers a larger interfacial area through which the mechanoradicals can reach the aqueous phase. The efficiency of the spongy polymer are commensurate with those of typical power plants (30% to 40%) or wind turbines (35% to 50%), though significantly lower than, for example, typical electric motors (50–90%).^[24] Also, as the fractions of bonds that are broken in the polymer by one squeezing event are very small (approximately one in a million bonds, see Figure S8 in the Supporting Information), these efficiencies are, to a good approximation, the same over large numbers (in this study, at least hundreds) of compression/release cycles.

In summary, mechanochemical synthesis can produce up to tens of milligrams of H_2O_2 per one square meter of polymer from the expenditure of 1 J and with an efficiency of mechanical-to-chemical energy conversion as high as 30%. Whereas the amounts of H_2O_2 that are obtained in our experiments are much smaller than in industrial syntheses of H_2O_2 , polymeric radical sponges can be used as environmentally clean, solid-state reagents to drive laboratory-scale, aqueous-phase, radical reactions. On the other hand, our results suggest that when polymeric materials are implanted in the human body (for example, siloxane-based breast implants), their mechanical deformations can generate harmful free radicals. In such cases, doping the polymers with free-radical scavengers (for example, with vitamin E) might reduce the health risks^[8,9] involved.

Received: November 17, 2011

Revised: February 2, 2012

Published online: March 1, 2012

Keywords: hydrogen peroxide · mechanochemistry · polymer chemistry · radicals

- [1] a) H. Staudinger, E. O. Leupold, *Ber. Dtsch. Chem. Ges.* **1930**, 63, 730–733; b) H. Staudinger, W. Heuer, *Ber. Dtsch. Chem. Ges.* **1934**, 67, 1159–1164.
- [2] G. Kaupp, *CrystEngComm* **2009**, 11, 388–403.
- [3] a) M. K. Beyer, H. Clausen-Schaumann, *Chem. Rev.* **2005**, 105, 2921–2948; b) W. D. Potter, G. Scott, *Eur. Polym. J.* **1971**, 7, 489–497; c) R. S. Porter, A. Casale, *Polym. Eng. Sci.* **1985**, 25, 129–156.
- [4] a) M. Pike, W. F. Watson, *J. Polym. Sci.* **1952**, 9, 229–251; b) D. J. Harmon, H. L. Jacobs, *J. Appl. Polym. Sci.* **1966**, 10, 253–257; c) J. L. Leblanc, R. Lionnet, *Polym. Eng. Sci.* **1992**, 32, 989–997.
- [5] a) R. M. van den Einde, C. Akkermans, A. J. van der Goot, R. M. Boom, *Carbohydr. Polym.* **2004**, 56, 415–422; b) R. M. van den Einde, A. J. van der Goot, R. M. Boom, *J. Food Sci.* **2003**, 68, 2396–2404; c) M. Kuzuya, Y. Yamauchi, S.-i. Kondo, *J. Phys. Chem. B* **1999**, 103, 8051–8059.
- [6] V. Birke, J. Mattik, D. Runne, *J. Mater. Sci.* **2004**, 39, 5111–5116.
- [7] D. A. Davis, A. Hamilton, J. Yang, L. D. Cremer, D. Van Gough, S. L. Potisek, M. T. Ong, P. V. Braun, T. J. Martínez, S. R. White, J. S. Moore, N. R. Sottos, *Nature* **2009**, 459, 68–72.

- [8] B. Halliwell, J. M. C. Gutteridge, *Free Radicals in Biology and Medicine*, Oxford Science Publications, New York, **1999**.
- [9] E. D. Lykissa, S. V. Kala, J. B. Hurley, R. M. Lebovitz, *Anal. Chem.* **1997**, *69*, 4912–4916, and references therein.
- [10] S. H. Jeong, S. J. Hong, *J. Biochem. Mol. Biol.* **1995**, *28*, 293–300.
- [11] a) T. Yamane, K. Makino, N. Umezawa, N. Kato, T. Higuchi, *Angew. Chem.* **2008**, *120*, 6538–6540; *Angew. Chem. Int. Ed.* **2008**, *47*, 6438–6440; b) G. R. Buettner, *Free Radical Biol. Med.* **1987**, *3*, 259–303.
- [12] The ^1H NMR signal for H_2O_2 is between 10–11 ppm depending on its concentration. N. A. Stephenson, A. T. Bell, *Anal. Bioanal. Chem.* **2005**, *381*, 1289–1293.
- [13] The molar extinction coefficient of H_2O_2 is $200\text{ m}^{-1}\text{ cm}^{-1}$ at 200 nm. S. O. Nielsen, B. D. Michael, E. J. Hart, *J. Phys. Chem.* **1976**, *80*, 2482–2488.
- [14] F. Haber, J. Weiss, *Naturwissenschaften* **1932**, *20*, 948–950.
- [15] C. J. Collins, J. M. Gebicki, *Anal. Biochem.* **1999**, *273*, 143–148.
- [16] a) K. Fateh-Alavi, M. Gällstedt, U. W. Gedde, *Polym. Degrad. Stab.* **2001**, *74*, 49–57; b) K. Fateh-Alavi, M. E. Núñez, S. Karlsson, U. W. Gedde, *Polym. Degrad. Stab.* **2002**, *78*, 17–25.
- [17] a) E. A. Nikitina, V. D. Khavryutchenko, E. F. Sheka, H. Barthel, J. Weis, *J. Phys. Chem. A* **1999**, *103*, 11355–11365; b) S. N. Zhurkov, V. A. Zakrevskiy, V. E. Korsukov, V. S. Kuksenko, *J. Polym. Sci. Part A* **1972**, *10*, 1509–1520.
- [18] a) P. J. Butiagin, *Pure Appl. Chem.* **1972**, *30*, 57–76; b) J. Sohma, *Pure Appl. Chem.* **1983**, *55*, 1595–1601.
- [19] M. K. Singh, H. Pal, A. C. Bhasikuttan, A. V. Sapre, *Photochem. Photobiol.* **1998**, *68*, 32–38.
- [20] J. Sohma, *Colloid Polym. Sci.* **1992**, *270*, 1060–1065.
- [21] a) T. K. Sarma, D. Chowdhury, A. Paul, A. Chattopadhyay, *Chem. Commun.* **2002**, 1048–1049; b) B. R. Panda, A. Chattopadhyay, *J. Nanosci. Nanotechnol.* **2007**, *7*, 1911–1915.
- [22] a) M. M. Alnuaimi, M. A. Rauf, S. S. Ashraf, *Dyes Pigm.* **2007**, *72*, 367–371; b) S. N. Guha, P. N. Moorthy, J. P. Mittal, *J. Chem. Soc. Perkin Trans. 2* **1993**, 409–415.
- [23] L. Du, M. Li, S. Zheng, B. Wang, *Tetrahedron Lett.* **2008**, *49*, 3045–3048.
- [24] R. A. Hinrichs, M. H. Kleinbach, *Energy: Its Use and the Environment*, Brooks/Cole, New York, **2005**.
- [25] a) A. M. Dubinskaya, S. F. Nikul'shin, A. Y. Rabkii, B. G. Zavii, *Polym. Sci. U.S.S.R.* **1980**, *22*, 2212–2220; b) A. M. Dubinskaya, A. N. Streletski, *Polym. Sci. U.S.S.R.* **1982**, *24*, 2202–2210.
- [26] Bond dissociation energies for C–C and Si–O are 306 kJ mol^{-1} and 445 kJ mol^{-1} respectively.